Identification of a Determinant of Epidermal Growth Factor Receptor Ligand-Binding Specificity Using a Truncated, High-Affinity Form of the Ectodomain

Thomas C. Elleman,[‡] Teresa Domagala,[§,||] Neil M. McKern,[‡] Maureen Nerrie,[§,||] Björn Lönnqvist,[⊥] Timothy E. Adams,[‡] Jennifer Lewis,[‡,||] George O. Lovrecz,[‡,||] Peter A. Hoyne,[‡] Kim M. Richards,[‡] Geoffrey J. Howlett,[#] Julie Rothacker,[§,||] Robert N. Jorissen,[§,||] Meizhen Lou,[||,△] Thomas P. J. Garrett,[||,△] Antony W. Burgess,[§,||] Edouard C. Nice,*[,§,||] and Colin W. Ward*[,‡,||]

CSIRO Health Sciences and Nutrition, 343 Royal Parade, Parkville, Victoria 3052, Australia, Ludwig Institute for Cancer Research, P.O. Box 2008, Royal Melbourne Hospital, Parkville, Victoria 3050, Australia, School of Engineering, Uppsala University, Uppsala, Sweden, Department of Biochemistry, University of Melbourne, Parkville, Melbourne, Victoria 3052, Australia, Biomolecular Research Institute, 343 Royal Parade, Parkville, Victoria 3052, Australia, and Cooperative Research Centre for Cellular Growth Factors, Royal Melbourne Hospital, Parkville, Victoria 3050, Australia

Received January 4, 2001; Revised Manuscript Received May 3, 2001

ABSTRACT: Murine and human epidermal growth factor receptors (EGFRs) bind human EGF (hEGF), mouse EGF (mEGF), and human transforming growth factor α (hTGF-α) with high affinity despite the significant differences in the amino acid sequences of the ligands and the receptors. In contrast, the chicken EGFR can discriminate between mEGF (and hEGF) and hTGF-α and binds the EGFs with approximately 100-fold lower affinity. The regions responsible for this poor binding are known to be Arg^{45} in hEGF and the L2 domain in the chicken EGFR. In this study we have produced a truncated form of the hEGFR ectodomain comprising residues 1−501 (sEGFR501), which, unlike the full-length hEGFR ectodomain (residues 1−621, sEGFR621), binds hEGF and hTGF-α with high affinity (K_D = 13−21 and 35−40 nM, respectively). sEGFR501 was a competitive inhibitor of EGF-stimulated mitogenesis, being almost 10-fold more effective than the full-length EGFR ectodomain and three times more potent than the neutralizing anti-EGFR monoclonal antibody Mab528. Analytical ultracentrifugation showed that the primary EGF binding sites on sEGFR501 were saturated at an equimolar ratio of ligand and receptor, leading to the formation of a 2:2 EGF:sEGFR501 dimer complex. We have used sEGFR501 to generate three mutants with single position substitutions at Glu^{367}, Gly^{441}, or Glu^{472} to Lys, the residue found in the corresponding positions in the chicken EGFR. All three mutants bound hTGF-α and were recognized by Mab528. However, mutant Gly^{441}Lys showed markedly reduced binding to hEGF, implicating Gly^{441}, in the L2 domain, as part of the binding site that recognizes Arg^{45} of hEGF.

The epidermal growth factor receptor (EGFR)[1] family consists of four distinct tyrosine kinase receptors, EGFR/HER/ErbB1, HER2/Neu/ErbB2, HER3/ErbB3, and HER4/ErbB4 (*1*). These receptors are widely expressed in epithelial, mesenchymal, and neuronal tissues and play fundamental roles during development and differentiation (*1*). They are activated by a family of at least 12 different ligands that induce either homo- or heterodimerization of the EGFR homologues (*2*). Constitutive activation of these receptors through autocrine stimulation or other mechanisms is associated with many types of human cancer (*1*, *3*−*6*).

The EGFR is a large (1186 residues), monomeric glycoprotein with a single transmembrane region and a cytoplasmic tyrosine kinase domain flanked by noncatalytic regulatory regions. Sequence analyses have shown that the ectodomain (residues 1−621) contains four subdomains, here termed L1, CR1, L2, and CR2, where L and CR are acronyms for large and Cys-rich, respectively (*7*, *8*). These domains are also referred to as domains I−IV (*9*).

The high-affinity form of the EGFR ectodomain used in this study (sEGFR501) comprises the L1/CR1/L2 domains plus the first module of the second Cys-rich region CR2. Its design was based on the following information. First, a shorter construct, sEGFR476, comprising the L1/CR1/L2 domains only, failed to bind ligand, suggesting that additional

* Corresponding authors. C.W.W.: CSIRO Health Sciences and Nutrition, 343 Royal Parade, Parkville, Victoria 3052, Australia. Phone: 61 3 9662 7291. Fax: 61 3 9662 7101. E-mail: Colin.Ward@hsn.csiro.au. E.C.N.: Ludwig Institute for Cancer Research, P.O. Box 2008, Royal Melbourne Hospital, Parkville, Victoria 3050, Australia. Phone: 61 3 9341 3155. Fax: 61 3 9347 1938. E-mail: ed.nice@ludwig.edu.au.

[‡] CSIRO Health Sciences and Nutrition.

[§] Ludwig Institute for Cancer Research.

[||] Royal Melbourne Hospital.

[⊥] Uppsala University.

[#] University of Melbourne.

[△] Biomolecular Research Institute.

[1] Abbreviations: CHO, Chinese hamster ovary; DMEM, Dulbecco's modified Eagle's medium; EGF, epidermal growth factor; EGFR, epidermal growth factor receptor; FCS, fetal calf serum; IGF-1R, insulin-like growth factor type 1 receptor; MSX, methionine sulfoximine; TGF-α, transforming growth factor α; PCR, polymerase chain reaction; sEGFR501, residues 1−501 of the human EGFR ectodomain; sEGFR621, whole human EGFR ectodomain (residues 1−621); Mab, monoclonal antibody.

10.1021/bi010037b CCC: $20.00
Published on Web 07/03/2001

regions of the receptor were required. Second, the structure of the L1/CR/L2 fragment of the related IGF-1R showed that a conserved tryptophan residue, Trp^{176}, in the first module of the Cys-rich region, is inserted between the last two rungs of the L1 domain (*10*). An equivalent tryptophan residue, Trp^{492}, and hydrophobic pocket are preserved in the first module of the second Cys-rich region of EGFR and the L2 domain of EGFR, respectively, but not in the L2 domains of IGF-1R and IR, which lack a second Cys-rich region (*10*). Third, the normal ligand binding and signaling properties of an 83 amino acid (residues 521−603) deletion mutant of EGFR from a human glioma (*11*) indicated that much of the CR2 domain (domain IV) could be removed without detriment. Finally, the 40 kDa, proteolytically derived, EGFR fragment (residues 302−503), which is capable of binding EGF with a K_D of approximately 1 μM, also includes the first module of CR2 (*12*). Taken together, these observations suggest that interactions between the first Cys-rich module of CR2 and the L2 domain may be important in maintaining the structural integrity of the EGFR.

Murine and human EGFRs bind hEGF, mEGF, and hTGF-α with high affinity despite the significant differences in the sequences of the ligands and the receptors (*13*−*15*). In contrast, chicken EGFR binds hEGF with approximately 100-fold lower affinity than hTGF-α (*9*). The region on hEGF responsible for reduced binding to the chicken receptor is Arg^{45} (*16*, *17*), while the region of the chicken receptor responsible for this differential recognition is contained within Lys^{301}−Asp^{484} (mature receptor numbering) in the L2 domain (*18*). The low binding of hEGF was suggested to result from electrostatic repulsion by positively charged residues close to, or within, the ligand binding domain of the chicken receptor but absent from the human or mouse receptors (*17*).

In the present study, the binding properties of sEGFR501, including its ability to form ligand-induced dimers and to act as an inhibitor of the EGF-stimulated mitogenic responses of BaF/3 cells transfected with the EGFR, have been characterized. sEGFR501 bound ligand with high affinity, comparable to that observed with detergent extracts of cell membranes (*15*), the chemically cross-linked dimer of full-length soluble ectodomain (sEGFR621) (*19*−*21*), or the higher affinity form of sEGFR621 present as a minor component in recombinant CHO cell-derived receptor (*22*). In addition, DNA encoding this truncated, high-affinity EGFR was used to generate three L2 domain mutants with single substitutions at Glu^{367}, Gly^{441}, or Glu^{472} to Lys, the residue found at the corresponding position in the chicken EGFR. A molecular model of the EGFR ectodomain (*23*), based on the 3D structure of the IGF-1R (*10*), indicates that two of these residues, 441 and to a lesser extent 472, lie close to Lys^{465}, a residue shown to be in close proximity to Arg^{45} of EGF in the complex by chemical cross-linking (*24*). The third mutant, at residue 367, was examined because previously it had been suggested (*17*) to be a likely candidate for ligand interaction on the basis of its close proximity to the epitope (residues 351−364) for the ligand-competitive monoclonal antibodies LA22, LA58, and LA90 (*25*). Only one mutant, Gly^{441}Lys, resembled chicken EGFR (*9*, *14*, *18*) in showing differential binding of hTGF-α and hEGF.

EXPERIMENTAL PROCEDURES

Construction of Plasmids Used for the Expression of Truncated Forms of the hEGFR Ectodomain. The plasmid pEGFR used in the construction of truncated hEGFR cDNAs comprised nucleotides 167−3970 of hEGFR (*13*) in the multiple cloning site of plasmid pUC18. Coding was in the opposite sense to the LacZ α peptide, and the insertion was downstream of the *Xba*I site of pUC18, which was used later in excision of the truncated constructs for insertion into the mammalian expression vector pEE14 (*26*).

Construction of pEGFR476. An initial plasmid containing nucleotides 167−3150 of hEGFR was constructed by ligation of a *Xba*I/*Nsi*I fragment from pEGFR and *Xba*I/*Pst*I-cut pBluescript KS+. From this plasmid, a 4 kbp *Bbs*I/*Bgl*II fragment (containing all of pBluescript KS+ and nucleotides 167−1150 and 2951−3150 of EGFR) and a 528 bp *Bbs*I/*Pvu*II fragment (nucleotides 1151−1679) were ligated with a 70 bp PCR-derived *Pvu*II and *Bgl*II fragment, encoding amino acids 474−476 of hEGFR, an enterokinase cleavage site, and a c-myc epitope tag to facilitate purification. The 70 bp PCR cassette was produced using a similar previous construct (*27*) as template. A plasmid for mammalian cell transfection, pEGFR476, was constructed from this plasmid by ligation of a 1.6 kbp *Xba*I/*Eco*RV fragment with *Xba*I/*Sma*I-cut pEE14.

Construction of pEGFR501 and pEGFR513. In each construction PCR was used with three oligonucleotides to produce a fragment of hEGFR cDNA (nucleotides 1121−1760 or 1121−1797, respectively), followed by a sequence which encoded an enterokinase cleavage site, a c-myc epitope tag, and a termination codon. The upstream primer in PCR corresponded to an arbitrary choice of nucleotides 1121−1140 of hEGFR cDNA, while two overlapping downstream primers were used to construct an additional sequence adjacent to nucleotide 1760 or 1797, respectively. The PCR products were cloned using the pCR-Script vector (Stratagene). In each case this allowed an *Apa*I fragment harboring the newly constructed sequence beginning at nucleotide 1738 of hEGFR to be excised for subsequent insertion into the large *Apa*I fragment of pEGFR (which included the entire pUC18 sequence with hEGFR cDNA to nucleotide 1737) to prepare a plasmid encoding a truncated hEGFR with *Xba*I restriction sites adjacent to the coding sequence. From these pUC18-based plasmids the fragments harboring the truncated hEGFR cDNAs were excised by *Xba*I digestion and inserted into plasmid pEE14 at the *Xba*I site to prepare plasmids pEGFR501 and pEGFR513, respectively, for mammalian cell transfection.

Mutagenesis. The 1.7 kbp fragment harboring the truncated hEGFR cDNA of pEGFR501 was introduced into M13mp18 (*28*) for mutagenesis. Oligonucleotide-directed in vitro mutagenesis, using the USB-T7 Gen in vitro mutagenesis kit, was employed to produce three single site mutants of the truncated human sEGFR501 ectodomain, with residues Glu^{367}, Gly^{441}, and Glu^{472}, respectively, mutated to Lys to match the corresponding residues in chicken EGFR (*9*). Clones incorporating the mutations were identified by colony hybridization (*29*) using ^{32}P-labeled mutagenic oligonucleotide as a probe, and the mutations were confirmed by DNA sequence analysis (*30*). Vehicles for mammalian cell expression were generated for each mutant by excising the 1.7 kbp

fragment harboring the mutated sEGFR501 cDNA from M13 RF-DNA by *Xba*I digestion and inserting it into plasmid pEE14 (*26*) at the *Xba*I site.

Cell Culture, DNA Transfection, and Protein Analysis. For transient transfection assays, human 293T fibroblasts maintained in DMEM plus 10% fetal calf serum (FCS) were transfected with plasmid DNA using FuGENE (Roche Molecular Biochemicals, Sydney, NSW) according to the manufacturer's instructions. Supernatants were harvested 48 h after transfection, and cell lysates were prepared in NP-40 lysis buffer (*31*). To characterize secreted EGFR mutants, aliquots of supernatant and lysate were immunoprecipitated with a monoclonal antibody (9E10) to the c-myc tag or with Mab 225 (HB-8508, American Type Culture Collection), a conformationally dependent monoclonal antibody recognizing the extracellular domain of the hEGFR (*32*). Immune complexes were collected on protein A−Sepharose beads (Zymed Laboratories, Bioscientific Pty. Ltd., Gymea, NSW), fractionated by SDS−polyacrylamide gel electrophoresis (10% gel), and transferred to nitrocellulose membranes (*31*). Truncated hEGFR ectodomains and mutants were identified by probing membranes with horseradish peroxidase (HRP) conjugated Mab9E10 (Roche), followed by chemilumiscent detection with Pierce Super Signal substrate.

Stable cell lines expressing sEGFR501 were established in the Lec8 mutant cell line from CHOK (*33*) using glutamine synthetase as a selectable marker (*27*). Supernatants from methionine sulfoximine (MSX) resistant cell colonies were screened for secreted receptor by biosensor analysis (see below) or by dot blotting onto nitrocellulose and probing with HRP-Mab9E10. A single cell line was selected for cloning by limiting dilution.

Lec8 cells expressing sEGFR501 protein were cultured in a Celligen Plus bioreactor (New Brunswick Scientific, NJ) using 70 g of Fibra-Cell Disk carriers with 1.7 L of working volume. Continuous perfusion culture using glutamine-free DMEM/F12 medium supplemented with nonessential amino acids, nucleosides, and 10% FCS was maintained for 6 weeks. Selection pressure was maintained with 25 μM MSX for the duration of the fermentation. Perfusion rate was adjusted as required to ensure a residual glucose level of 1.0−1.5 g/L, with a corresponding lactate concentration of 2.0−2.3 g/L.

Purification of Truncated EGFR Ectodomains. For biosensor and AUC analyses, conditioned medium containing the sEGFR truncated proteins (4 L) was adjusted to pH 8.0 with Tris-HCl (Sigma) containing sodium azide [0.02% (w/v)] (TBSA), and particulates were removed by centrifugation prior to recovery of c-myc-tagged protein by affinity purification at 4 °C on a column of monoclonal antibody 9E10 covalently bound to agarose, using peptide elution (*27*). Eluted protein was further purified by size exclusion chromatography on Superdex 200 (HR10/30, Amersham Pharmacia Biotech) at room temperature using TBSA buffer at a flow rate of 0.8 mL/min. Protein was detected by absorbance at 280 nm.

BIAcore Binding Assays. Protein−protein interactions were monitored in real time on an instrumental optical biosensor using surface plasmon resonance detection (BIAcore 2000 or 3000, BIAcore, Uppsala, Sweden). Recombinant hEGF or hTGF-α (Gropep, Adelaide, Australia) were purified immediately prior to immobilization by micropreparative RP-HPLC using a SMART system (Amersham Pharmacia Biotech) as described previously (*34*). The proteins were immobilized onto the biosensor surface using amine coupling chemistry (*N*-hydroxysuccinimide and *N*-ethyl-*N*′-dimethylaminopropylcarbodiimide) at a flow rate of 4 μL/min. Typically 100−200 RU were immobilized equivalent to 0.1−0.2 ng/mm^2 (*34*). Automated targeting of immobilization levels was achieved using the BIAcore 3.1 control software (*35*).

Prior to analysis, sEGFR621 (*22*), sEGFR501, and the sEGFR501 mutant samples were characterized by micropreparative size exclusion chromatography (Superose 12 3.2/30, Amersham Pharmacia Biotech) to ensure size homogeneity (*34*), and pooled fractions were diluted in BIAcore buffer [HBS: 10 mM Hepes, pH 7.4, containing 3.4 mM EDTA, 0.15 mM NaCl, and 0.005% (v/v) Tween 20] to the appropriate concentration. Typically, samples (30 μL) at concentrations of 10−1000 nM were injected sequentially over the sensor surfaces at a flow rate of 5 or 10 μL/min. Following completion of the injection phase, dissociation was monitored in BIAcore buffer at the same flow rate. The sensor surface and sample blocks were maintained at 25 °C. Bound receptor was eluted, and the surface regenerated between injections, using 40 μL of 10 mM HCl. This treatment did not denature hEGF or hTGF-α immobilized onto the sensor surface, as shown by equivalent signals on reinjection of receptor.

Kinetic rate constants (k_a, k_d) were determined using the BIAevaluation 3.02 software (BIAcore, http//www.biacore-.com/products/eval3.html) as described previously (*36*) or by global analysis using CLAMP (*22*, *37*). Equilibrium binding constants (K_A, K_D) were determined by direct nonlinear least-squares analysis of the binding data using an equation defining steady-state equilibrium [$K_A \times$ concn $\times R_{max}/(K_A \times$ concn $\times n)$; BIAevaluation 3.1]. The data were also plotted in Scatchard format (R_{eq}/nC versus R_{eq}, where R_{eq} is the biosensor response at equilibrium, n is the valency, and C is the concentration) (*38*).

Analytical Ultracentrifugation. Experiments were performed using a Beckman XL-A analytical ultracentrifuge (Beckman Coulter, Inc., Fullerton, CA) equipped with absorption optics, using an An60-Ti rotor with cells containing quartz windows, as described previously (*22*). Centrifugation experiments were conducted at 20 °C using a sample volume of 100 μL. Equilibrium sedimentation distributions obtained at 12 000 and 20 000 rpm, were monitored at 280 or 290 nm and analyzed using the program SEDEQ1B (*39*). The partial specific volume of EGF was taken as 0.71 mL/g (*22*).

Chemical Cross-Linking. Chemically cross-linked sEGFR501 dimers were generated by the incubation of sEGFR501 (5 μM) with mEGF (20 μM) in 20 mM HEPES, pH 7.4, containing 150 mM NaCl for 1 h at room temperature followed by the addition of bis(sulfosuccinimidyl) suberate (BS3, Pierce, Rockford, IL) to a final concentration of 0.5 mM and incubation for a further 30 min. The reaction was terminated by the addition of Tris-HCl buffer (pH 7.5) to a final concentration of 10 mM. Monomer−dimer separation was achieved on Novex nonreducing SDS−PAGE gels (10%). Proteins were transferred onto poly(vinyl difluoride) (PVDF) membranes (Bio-Rad, Hercules, CA) and identified by incubation with anti-EGFR Mab528 (*32*) (0.5 μg/mL)

followed by horseradish peroxidase-labeled goat anti-mouse IgG (Bio-Rad) and ECL detection (Amersham Pharmacia Biotech).

Cell Proliferation Assays. BaF/3ERX cells, a cell line derived from BaF/3 cells transfected with human EGFR (a gift from Dr. F. Walker, Ludwig Institute for Cancer Research, Melbourne), were washed three times to remove residual IL-3 and resuspended in RPMI 1640 plus 10% FCS. Cells were seeded into 96-well plates using a Biomek 2000 robotic autosampler (Beckman) at 2×10^4 cells per 200 μL and incubated for 4 h at 37 °C in 10% CO_2. Appropriate concentrations of sEGFR501 or sEGFR621 or the anti-EGFR monoclonal antibody Mab528 were added to the first titration point and titrated in 2-fold dilutions across the 96-well plate in duplicate with or without a constant amount of mEGF (207 pM). [^{3}H]Thymidine (0.5 μCi/well) was added, and the plates were incubated for 20 h at 37 °C in 5% CO_2. The cells were then lysed in 0.5 M NaOH at room temperature for 30 min before being harvested onto nitrocellulose filter mats using an automatic harvester (Tomtec, CT). The mats were dried in a microwave and placed in a plastic counting bag, and scintillant (10 mL) was added. [^{3}H]Thymidine incorporation was determined using an automated beta counter (1205 Betaplate, Wallac, Finland).

RESULTS

Production and Purification of Truncated EGFR Ectodomains. Preliminary analysis of conditioned media from cells transiently expressing sEGFR476, sEGFR501, and sEGFR513 showed that only the latter two truncated receptors gave detectable binding to hEGF immobilized on the BIAcore biosensor (data not shown). Stably transfected Lec8 cells expressing sEGFR501 were generated and used to produce truncated receptor protein at a yield of ~1.8 mg/L of fermentation medium for physical−chemical characterization.

sEGFR501 purified from a Mab9E10 anti-c-myc peptide affinity column using peptide elution showed a single symmetrical peak on size exclusion chromatography (apparent molecular mass of ~80 kDa) and migrated as a single band of ~70 kDa on SDS−PAGE under reducing conditions (not shown). sEGFR501 gave a unique expected sequence, LEEKKVXQGT (*13*), on N-terminal amino acid sequence analysis, the X at cycle 7 being due to the presence of a disulfide-bonded cysteine residue at that position. The apparent molecular mass of 70 kDa on SDS−PAGE is due to the residual glycosylation reported for the glycosylation-defective Lec 8 cells (*33*) since the calculated mass of human sEGFR501 apoprotein is ~57.5 kDa. There are eight potential N-linked glycosylation sites in sEGFR501 (*13*), and incubation of sEGFR501 with peptide *N*-glycosidase (PNGase) at 37 °C resulted in the generation of a major band migrating on SDS−PAGE with an apparent molecular mass of 57−58 kDa (data not shown). We have shown previously using BIAcore analysis (*21*) that removal of carbohydrate using PNGase does not affect binding of sEGFR621 to the immobilized ligand, in agreement with the concept that glycosylation is required for correct processing but not for biological activity (*40*). All subsequent experiments were carried out using the 70 kDa sEGFR501.

sEGFR501 Shows Higher Affinity Binding Than sEGFR621. The BIAcore biosensor was used to determine both the rate and equilibrium binding constants for the interaction between sEGFR501 and hEGF or hTGF-α. Full-length ectodomain (sEGFR621) was used as a positive control for the surface reactivity, since this interaction has been studied in detail previously (*20*, *22*, *41*).

Representative sensorgrams for the interaction between sEGFR501 or sEGFR621 and hEGF or TGF-α are shown in Figure 1. Visual inspection revealed that the curves approached equilibrium over the concentration ranges tested. Additionally, the hTGF-α sensorgrams appeared to show more rapid, and virtually complete, dissociation. Thermodynamic analysis of the equilibrium binding data in Scatchard format (Figure 2) indicated K_D values of 30 and 47 nM (correlation coefficient $R = 0.993$ and 0.999, respectively) for the interactions between sEGFR501 and immobilized hEGF or hTGF-α and 412 and 961 nM ($R = 0.997$ and 0.999, respectively) for the corresponding interactions with sEGFR621. The values obtained by Scatchard transformation were also confirmed by direct nonlinear least-squares analysis of the binding data (data not shown) using an equation defining steady-state equilibrium ($K_A \times \text{concn} \times R_{max}/(K_A \times \text{concn} \times n)$; BIAevaluation 3.1). Using this analysis, K_D values of 32 and 46 nM were calculated for the interaction between sEGFR501 and immobilized hEGF and hTGF-α, respectively, and 570 and 959 nM for the interaction between full-length ectodomain (sEGFR621) and immobilized hEGF and hTGF-α. The values obtained with sEGFR621 were in good agreement with those reported previously (*20*, *22*, *41*), confirming the surface viability.

The individual rate constants were determined from those parts of the curves where first-order kinetics appeared to be operative **(***41*, *42***)** and the corresponding dissociation constants calculated (Table 1). Again, there was good agreement between the K_D values calculated in this manner and those obtained from the equilibrium binding data. It is interesting to note that the binding curves obtained with both sEGFR501 and sEGFR621 for hTGF-α appeared to be better fitted to a 1:1 model than the corresponding data for the hEGF surface (as suggested by the virtually complete dissociation).

sEGFR501 Exhibits Strong Antagonist Activity. The observation that sEGFR501 bound EGF with high affinity prompted us to test whether sEGFR501 would act as a competitive inhibitor for the mitogenic stimulation of EGFR in a cell-based assay using the BaF/3ERX cell line. This cell line responds to mEGF with an EC_{50} of approximately 30 pM (Figure 3A). The competition assay (Figure 3B) used a constant concentration of mEGF (207 pM), which causes maximal stimulation (Figure 3A), and varying levels (0.00045−0.5 μM) of sEGFR501, sEGFR621, or the neutralizing anti-EGFR monoclonal antibody Mab528 raised against epidermal growth factor receptors on a human epidermoid carcinoma cell line, A431 (*32*). This antibody has been shown to prevent the growth of A431 cell xenografts, bearing high numbers of EGF receptors, in nude mice (*43*). The sEGFR501 ($IC_{50} = 0.02$ μM) was almost 10-fold more potent than the full-length ectodomain ($IC_{50} = 0.15$ μM) and approximately 3-fold more potent than the Mab528 anti-EGFR monoclonal antibody ($IC_{50} = 0.06$ μM).

sEGFR501 Forms 2:2 Dimers in the Presence of Ligand. Chemical cross-linking revealed that sEGFR501 formed dimeric complexes in the presence of ligand. In the presence of 20 μM mEGF, a single high molecular weight species

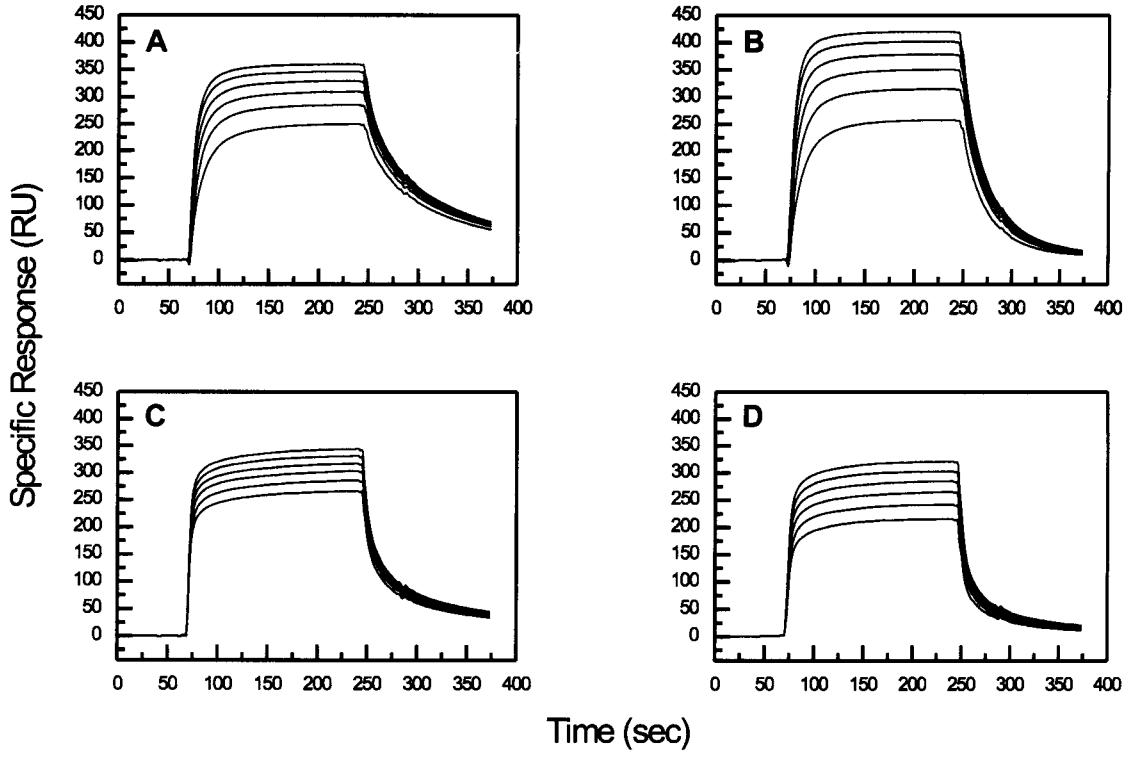

FIGURE 1: BIAcore analysis of the interactions between sEGFR501 and sEGFR621 with immobilized hEGF or hTGF-α. (A) sEGFR501 (140, 120, 100, 80, 60, and 40 nM) was passed over immobilized hEGF (160 RU immobilized). Samples (30 μL) were injected at a flow rate of 10 μL/min. (B) sEGFR501 was passed over immobilized hTGF-α (132 RU immobilized). Experimental details were as in panel A. (C) sEGFR621 (1000, 900, 800, 700, 600, and 500 nM) was passed over immobilized hEGF. (D) EGFR621 (concentrations as for panel C) was passed over immobilized hTGF-α. The operating temperature was 25 °C. At the end of the injection phase, dissociation was monitored with buffer alone flowing over the sensor surface. The surface was regenerated between samples using 10 mM HCl. The signal obtained when the sample was passed over a parallel blank channel has been subtracted electronically to give the specific response.

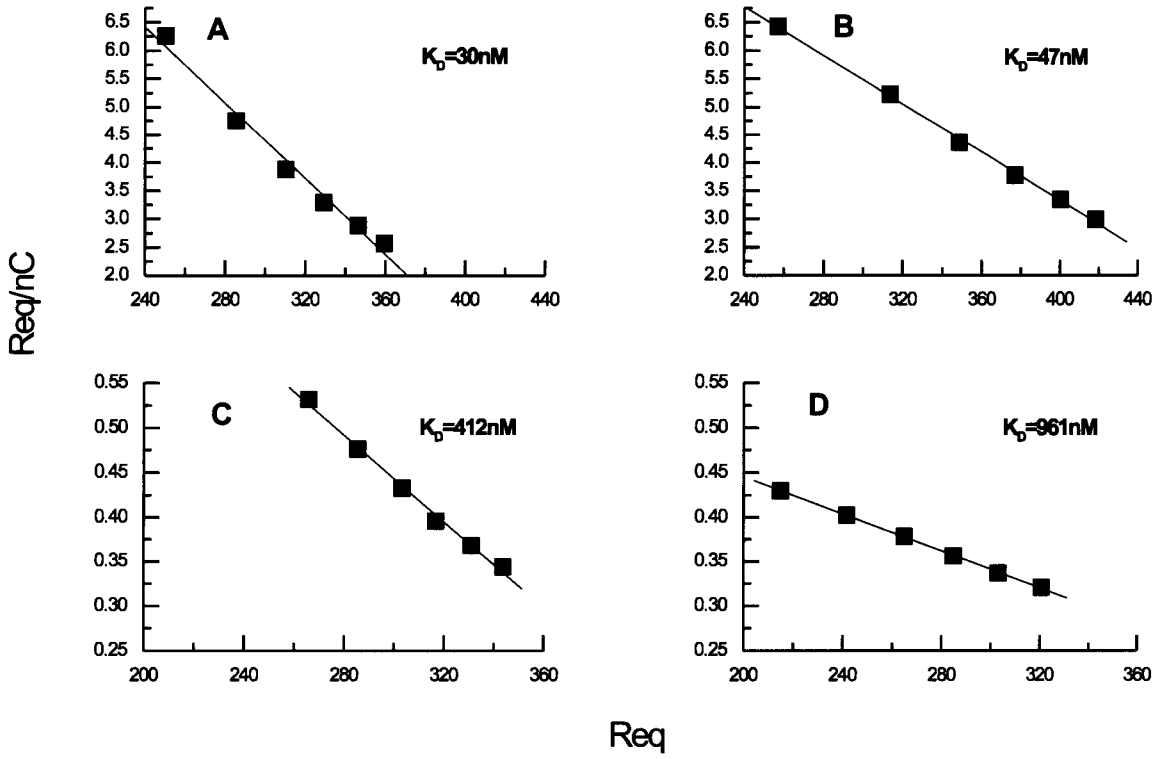

FIGURE 2: Scatchard analysis of equilibrium binding data. The dissociation constant ($K_D = 1/K_A$) was calculated from the equilibrium binding response obtained in Figure 1 by plotting the data in Scatchard format (R_{eq}/nC versus R_{eq}; see Experimental Procedures). The slope of the linear fit to the data gives K_A. (A) sEGFR501 versus hEGF; (B) sEGFR501 versus hTGF-α; (C) sEGFR621 versus hEGF; (D) sEGFR621 versus hTGF-α.

(apparent M_r 180 000) was formed after chemical cross-linking which was not detectable when the cross-linking was attempted in the absence of ligand (Figure 4). Western blotting was employed to confirm the authenticity of the

Table 1: Comparative Kinetic Data for Ligand Binding by Truncated and Full-Length EGFR Ectodomains

interaction	k_a (M^{-1} s^{-1}) × 10^{-5}	k_d (s^{-1})	K_D (nM)
sEGFR501/EGF	10−17	0.02	13−21
sEGFR501/TGF-α	9.3−10.5	0.04	35−40
sEGFR621/EGF	2.9−4.8	0.08	180−300
sEGFR621/TGF-α	0.7−1.0	0.08	840−1320

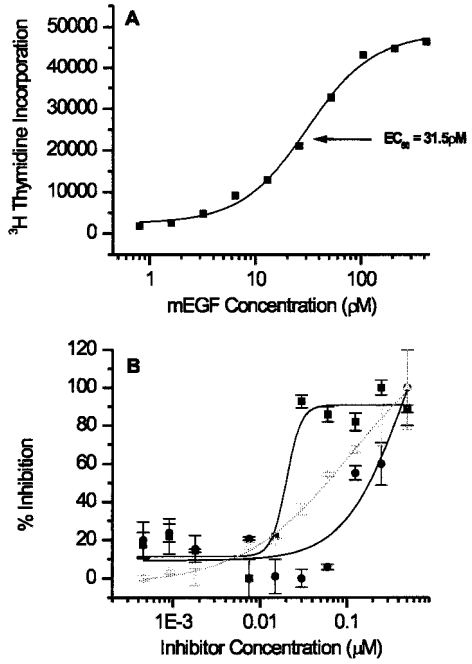

FIGURE 3: Inhibition of EGF-stimulated cell mitogenesis by sEGFR501. (A) Stimulation of [^{3}H]thymidine incorporation by BaF/3ERX cells using serial dilutions of mEGF. The data were fitted by a sigmoidal function (—) to determine the EC_{50}. (B) Inhibition of the mitogenic response of BaF/3ERX cells stimulated with mEGF (207 pM) by sEGFR501 (■), sEGFR621 (●), or anti-EGFR antibody Mab528 (▲). Each point was assayed in triplicate. Error bars are shown.

bands observed, but similar data were obtained with silver or Coomassie blue staining. In addition, size exclusion chromatographic analysis of the reaction mixture, using a TSK G2000SW column developed with a mobile phase of PBS at a flow rate of 0.25 mL/min, showed a peak of apparent M_r 158 000 which corresponded to dimer (data not shown). Similar results were obtained with sEGFR621 (*21*).

Analytical ultracentrifugation showed that the EGF binding sites on sEGFR501 were saturated at an equimolar ratio of ligand and receptor, leading to the formation of a 2:2 EGF/sEGFR501 complex (Figure 5). The data for 20 μM EGF alone (Figure 5A) indicate a single solute of molecular weight 5980, in good agreement with the value calculated from the amino acid composition (6040). The molecular weight (65 600) and partial specific volume (0.71 mL/g) determined for 10 μM sEGFR501 alone were calculated from the sedimentation equilibrium distribution (Figure 5A) and are based on the known amino acid composition and a calculated value of 12% (w/w) for the carbohydrate composition.

Sedimentation equilibrium data for a mixture of EGF (20 μM) and sEGFR501 (10 μM) were analyzed assuming two species (Figure 5A). The molecular weight of the first species was fixed at the value obtained for free EGF (6000) with the molecular weight and weight fraction of the second

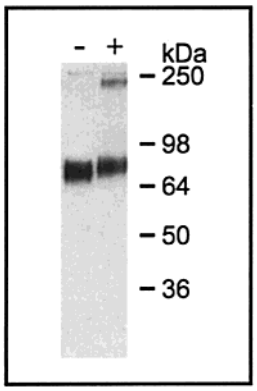

FIGURE 4: Covalent cross-linking of sEGFR501 dimers after incubation with mEGF. sEGFR501 (5 μM) was incubated with (+) or without (−) mEGF (20 μM) in 20 mM HEPES (pH7.4) containing 150 mM NaCl for 1 h at room temperature followed by the addition of bis(sulfosuccinimidyl) suberate (BS3, Pierce, Rockford, IL) to a final concentration of 0.5 mM and incubation for a further 30 min. The reaction was terminated, and the degree of dimer formation was monitored by SDS−PAGE and immunoblotting with anti-EGFR Mab528 (*32*) (0.5 μg/mL) and horseradish peroxidase-labeled goat anti-mouse IgG (Bio-Rad) with detection by ECL (Amersham Pharmacia Biotech). Analysis by nonreducing SDS−PAGE was necessary since the antibody used to detect sEGFR501 (Mab528) is conformation-dependent.

species used as fitting parameters. Under these conditions the molecular weight of the second species provides a good approximation to the weight-average molecular weight of sEGFR501 and its complexes. The best-fit value showed a complex of weight-average MW 106 400, higher than predicted for a 1:1 complex (71,600) and more consistent with the formation of a significant proportion of dimeric 2:2 EGF/sEGFR501 complex (see below).

High-speed meniscus depletion experiments were performed to determine the molar ratio required for saturation of sEGFR501 with EGF (Figure 5B). A solution of sEGFR501 (5 μM) was titrated with EGF to determine the molar ratio at which free EGF is detectable at the meniscus. The results show that this occurs above 5 μM EGF, implying that an equimolar ratio is required for saturation of the EGF binding site(s) on sEGFR501. These data, taken together with the observed weight-average molecular weight of the EGF/sEGFR501 complex obtained from the equilibrium analysis (Figure 5A), confirm that the stoichiometry of the EGF/sEGFR501 dimeric species is 2:2 not 2:1.

Sedimentation equilibrium was used for the analysis of data obtained for sEGFR501 (5 μM) in the presence of a range of EGF concentrations (Figure 5C). The weight-average molecular weight obtained for the "second" species increases rapidly as the ratio of EGF/sEGFR501 is increased to 1:1 and then tends to plateau around approximately 108 000 at ratios above 2:1 (Figure 5C). The data in Figure 5A could also be fitted assuming a mixture of 1:1 and 2:2 complexes with weight fractions of the monomeric and dimeric sEGFR501 complexes of 57% and 31%, respectively. Similar data were obtained with sEGFR621 (*22*).

*The 441 Mutant of sEGFR501 Shows Differential Binding of hEGF and hTGF*α. Biosensor analysis was also used to analyze the binding of the transiently expressed sEGFR501 mutants to both immobilized hEGF and hTGF-α surfaces. The presence of the mutant proteins in culture supernatants from transfected cell lines was demonstrated by both

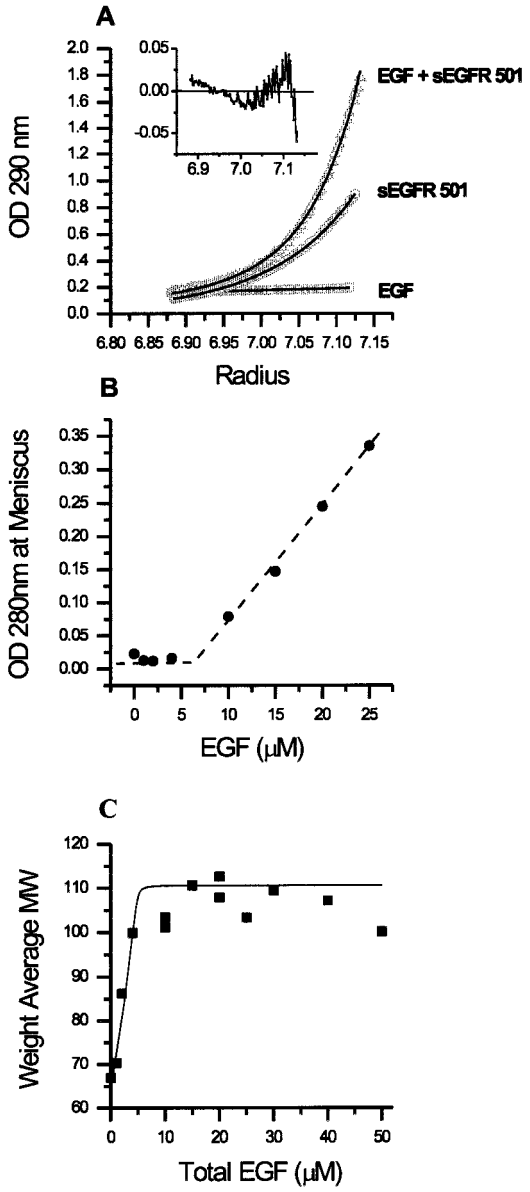

FIGURE 5: Analysis of EGF/sEGFR501 interactions using the analytical ultracentrifuge. (A) Sedimentation equilibrium analysis of EGF, sEGFR501, and a mixture of EGF and sEGFR501. The equilibrium distributions were obtained after centrifugation at 12 000 rpm at 20 °C for 16 h. Plots: (□) 20 μM EGF; (○) 10 μM sEGFR501; (△) 20 μM EGF + 10 μM sEGFR501. The lines of best fit drawn though the data for EGF and sEGFR501 are for single species and for molecular weight values of 6000 and 65 600, respectively. The line drawn through the data for the EGF/sEGFR501 mixture is the line of best fit calculated assuming two species with the molecular weight of the first species fixed at 6000 and a fitted value of 106 400 for the molecular weight of the second species. Inset: Residual plot for the fit of the EGF/sEGFR501 mixture. (B) Meniscus depletion sedimentation analysis of the stoichiometry of EGF binding to sEGFR501. Solutions containing 5 μM sEGFR501 and different molar ratios of EGF:EGFR were spun for 16 h at 20 000 rpm and 20 °C in the XLA analytical ultracentrifuge. Under these conditions sEGFR501 and its complexes with EGF are depleted from the meniscus leaving unbound EGF in the supernatant. Optical density measurements at 280 nm enable the amount of unbound EGF near the meniscus to be estimated. (C) Data obtained for the weight-average molecular weight of the "second" species calculated for mixtures of sEGFR501 (5 μM) and EGF at the concentrations indicated under the conditions of panel A above. The solid line corresponds to a simulated curve based on a K_D of 30 nM and a dimerization constant of 4 μM.

immunoblotting with the anti-EGFR monoclonal antibody, Mab528, and biosensor analysis using Mab528 immobilized on the surface. Culture supernatants from all cell lines showed demonstrable binding to the Mab surface (441 > 472 = wt > 367) (data not shown).

In preliminary experiments, the Glu^{367}Lys mutant and the Glu^{472}Lys mutant showed similar binding characteristics to sEGFR501 when passed over the hEGF sensor surface (data not shown). The Gly^{441}Lys mutant showed much reduced binding, even though the Mab528 surface had indicated that the Gly^{441}Lys mutant was present at higher concentrations than sEGFR501. Interestingly, when the same samples were passed over the parallel hTGF-α sensor surface, the Gly^{441}-Lys mutant now showed the highest binding, while the binding of the Glu^{367}Lys mutant, the Glu^{472}Lys mutant, and wild-type sEGFR501 were again similar but lower.

For full biosensor analysis the mutant proteins present in the conditioned media from transient transfected 293T fibroblasts were concentrated and purified by a combination of affinity purification using the 9E10 monoclonal antibody and size exclusion chromatography on Superdex 200 and Superose 12. The sensorgrams obtained with the immobilized hEGF and hTGF-α surfaces (160 and 132 RU immobilized, respectively) are shown in Figure 6A,B. As we had observed in the preliminary experiments, while the binding characteristics of the Glu^{367}Lys and Glu^{472}Lys mutants were essentially indistinguishable from those of sEGFR501 shown in Figure 1 (data not shown), the Gly^{441}Lys mutant again showed preferential binding to the hTGF-α surface (Figure 6A,B). Scatchard analysis of the equilibrium binding data (Figure 6C,D) indicated that while binding to the TGF-α surface was similar to that observed with sEGFR501 (K_D = 77 nM, correlation coefficient R = 0.999), the reactivity of the Gly^{441}Lys mutant toward the EGF surface was now considerably reduced (K_D = 455 nM, R = 0.995). Similar values (78 and 469 nM) were obtained by direct nonlinear least-squares analysis of the binding data (data not shown) using the equation defining steady-state equilibrium.

Kinetic analysis of the binding data (Table 2) indicated that the interaction with the immobilized TGF-α could be described by an association rate constant (k_a) of (5.2−6.9) × 10^{-5} M^{-1} s^{-1} and a dissociation rate constant (k_d) of 0.025 s^{-1}, giving a $K_D = k_d/k_a$ of 36−44 nM. The corresponding interaction with EGF was described by a k_a of (1.9−2.3) × 10^{-5} M^{-1} s^{-1} and a significantly faster k_d of 0.10 3 s^{-1}, giving a $K_D = k_d/k_a$ of 442−545 nM, in good agreement with the results observed from the thermodynamic analysis.

DISCUSSION

In this paper the characteristics of a truncated version of the EGFR ectodomain (sEGFR501) that binds hEGF and hTGF-α with high affinity (Table 1, Figures 1 and 2) are described. The K_D values of 13−21 nM for hEGF binding to sEGFR501 are similar to those (15−30 nM) seen with chemically cross-linked dimers of the full-length EGFR ectodomain (*19*, *20*, *21*) and are 10−25-fold higher than the values (150−400 nM) generally reported for the soluble, full-length EGFR ectodomain derived from either A431 tumor cells (*44*, *45*), transfected Sf9 insect cells (*19*, *45*, *46*), or CHO cells (*20*, *22*, *47*−*49*). Recently, it was shown that preparations of the full-length EGFR ectodomain produced

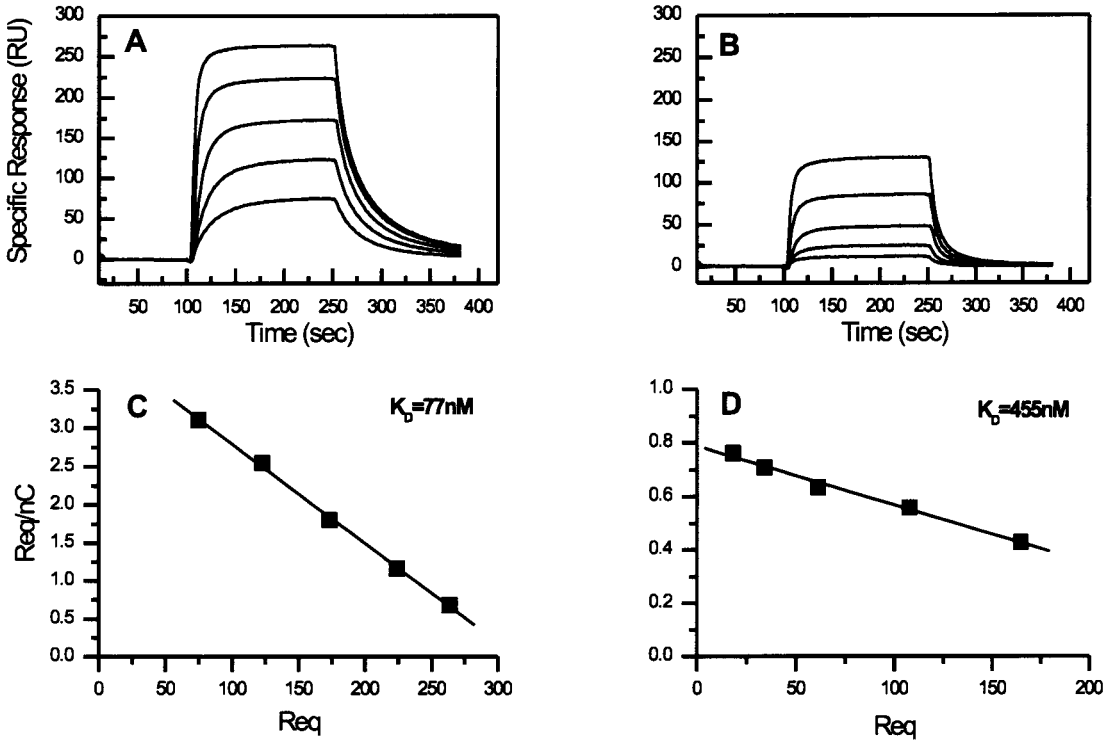

FIGURE 6: BIAcore analysis of the binding of the Gly[441]Lys sEGFR501 mutant to immobilized hEGF and hTGF-α. Purified Gly[441]Lys sEGFR501 (24−385 nM) was passed over immobilized hTGF-α (panel A) or hEGF (panel B) using the experimental conditions described in Figure 1. The corresponding Scatchard analysis, using the equilibrium binding values obtained from these sensorgrams, is shown below (panels C and D).

Table 2: Kinetic Analysis of the Binding of Gly[441]Lys sEGFR501 to Immobilized hEGF and hTGF-α

interaction	k_a (M^{-1} s^{-1}) × 10^{-5}	k_d (s^{-1})	K_D (nM)
TGF-α	5.2−6.9	0.025	36−48
EGF	1.9−2.3	0.103	442−545

in CHO cells contained two populations of molecules, one of which showed high affinity (K_D 1−20 nM) for hEGF and represented 10−15% of the total preparation (*22*). The nature of the higher affinity form, which has similar affinity to that observed with the truncated sEGFR501 described in this paper, was not established. However, in view of the current data it is possible that, in solution, the majority of the sEGFR621 is in a conformation where the CR2 domain, most of which is absent in sEGFR501, hinders complete binding. It has been suggested that the extracellular domain of the intact receptor may sterically inhibit dimerization in the absence of ligand (*50*).

The high-affinity binding of the truncated sEGFR501 suggests that the loss of EGF binding seen in the EGFR with multiple mutations (Glu[521]Ala, Arg[523]Ala, Glu[524]Ala, Phe[525]-Ala, Glu[527]Ala), in the third module of CR2 (domain IV) or after deletion of residues 518−589 (*51*), is due to indirect effects rather than a direct contribution to the ligand-binding pocket. Molecular modeling (*23*) indicates that the first module of CR2 (residues 480−501) is unlikely to make direct contact with ligand, since it is positioned away from the putative binding pocket and away from the face of the L2 domain implicated in ligand binding by chemical cross-linking studies (*24*).

sEGFR501, which lacks most of CR2, exhibits ligand-induced receptor dimerization (Figures 4 and 5), indicating that the regions responsible for dimerization are unlikely to include CR2. It also confirms that membrane anchoring is not required for the generation of high- affinity dimers in contrast to the situation with ErbB2/ErbB3 heterodimers and neuregulin (*52*). The ultracentrifugation analyses showed that the binding sites on sEGFR501 were saturated, and the extent of dimerization began to plateau at molar ratios greater than 1:1 (Figure 5C), even at the relatively low concentration of sEGFR501 of 5 μM (320 μg/mL). This compares favorably with the small-angle X-ray scattering data (*48*) and our previous analytical ultracentrifugation analyses (*22*) that showed that sEGFR621 dimerization, induced by EGF or TGF-α binding, reached a maximum when the ratio of EGF/sEGFR was 1:1.

The truncated receptor, sEGFR501, is a valuable reagent to further investigate the parameters involved in ligand binding and ligand-induced receptor homo- and heterodimerization. sEGFR501 also provides a new candidate for crystallization studies as it is composed of similar modules to, and is only slightly larger than, the fragment of the IGF-1R whose structure was recently solved by X-ray crystallography (*10*), and unlike the IGF-1R fragment, it binds ligand with high affinity. High-resolution data of ligand/receptor complexes will show how members of the EGFR family recognize and selectively bind multiple members of a highly variable family of ligands. Such information will aid the generation of EGFR antagonists for evaluation as potential anticancer therapeutics. sEGFR501 may itself have therapeutic potential, given its high affinity for ligand and its ability to competitively inhibit EGF-induced proliferation responses in a model cell system (Figure 3). This inhibition was greater than that achieved in the same assay with a neutralizing monoclonal antibody raised against the receptor (Mab528), chimeric forms of which (C225) are currently in

clinical trails (*53*).

sEGFR501 was also employed to investigate the residue responsible for the differential binding between hTGF-α and hEGF observed with chicken EGFR (*9*). The region on hEGF resulting in poor binding to the chicken receptor has been previously mapped to the C-terminal residues 43−53, by examining the binding properties of 10 hEGF/ hTGF-α chimeras (*16*). Subsequent analysis of a series of truncated ligands or multiple site/single site mutations showed that Arg^{45} was critically important (*17*). The single mutation Arg^{45}Ala was sufficient to confer high-affinity binding of hEGF to the chicken EGFR, suggesting that electrostatic repulsion by positively charged residues close to, or within, the ligand binding domain of the chicken receptor (but absent from the human or mouse receptors) was responsible for the poor binding (*17*).

The region of the chicken receptor responsible for discrimination between mEGF and hTGF-α has been shown to lie between residues Lys^{301}−Asp^{484} (mature receptor numbering) from an analysis of a series of chimeras of the human and chicken receptors (*18*). This region consists of the L2 domain plus some small flanking sequences and contains 49 amino acid sequence differences between the chicken and human receptors, six of which (equivalent to residues 340, 367, 420, 441, 472, and 479 in hEGFR) are basic residues not present in the human or mouse receptor.

Molecular modeling of the sEGFR (*23*) based on the 3D structure of the IGF-1R (*10*) indicated that residue 340 is positioned at the back of the L2 domain and is unlikely to contribute to binding, while residue 420 is part of a glycosylation site in hEGFR and is likely to be masked by carbohydrate. Residue 479 was not mutated since it lies between the end of the L2 domain and the first module of CR2 and appeared unlikely to be part of the binding site (*23*). The three residues mutated to lysine in this study were Glu^{367}, Gly^{441}, and Glu^{472}. Residue Glu^{367} is close to the epitope (residues 351−364) for three competitive antibodies, LA-22, LA-58, and LA-90 (*25*), and had been suggested as the most likely candidate for discrimination against hEGF by the chicken receptor (*17*).

The Glu^{367}Lys mutation had no effect on binding of either ligand. Gly^{441} and Glu^{472} are on the same face of the L2 domain as Lys^{465}, the residue labeled by chemically cross-linking an Arg^{45}Lys mutant of hEGF (*24*). While the Glu^{472}-Lys mutation also had no effect on ligand-binding characteristics, the Gly^{441}Lys mutation showed considerably reduced affinity for hEGF without compromising its affinity for hTGF-α (Figure 6). These data demonstrate that the Lys^{442} in chicken EGFR, which corresponds to Gly^{441} in hEGFR, is the residue responsible for discriminating between hTGF-α and hEGF binding.

REFERENCES

1. Burgess, A. W., and Thumwood, C. M. (1994) *Pathology 26*, 453−463.
2. Sundarasen, S., Roberts, P. E., King, K. L., Sliwkowski, M. X., and Mather, J. P. (1998) *Endocrinology 139*, 4756−4764.
3. Harris, A. L., Nicholson, S., Sainsbury, J. R. C., Neal, D., Smith, K., Farndon, J. R., and Wright, C. (1989) in *The molecular diagnostics of human cancer* (Furth, M., and Greaves, M., Eds.) pp 353−357, Cold Spring Harbor Laboratory Press, Cold Spring Harbor, NY.
4. Sandgreen, E. P., Luettke, N. C., Palmiter, R. D., Brinster, R. L., and Lee, D. C. (1990) *Cell 61*, 1121−1135.
5. Karnes, W. E. J., Walsh, J. H., Wu, S. V., Kim, R. S., Martin, M. G., Wong, H. C., Mendelsohn, J., Gazdar, A. F., and Cuttitta, F. (1992) *Gastroenterology 102*, 474−485.
6. Hines, N. E. (1993) *Semin. Cancer Biol. 4*, 19−26.
7. Bajaj, M., Waterfield, M. D., Schlessinger, J., Taylor, W. R., and Blundell, T. (1987) *Biochim. Biophys. Acta 916*, 220−226.
8. Ward, C. W., Hoyne, P. A., and Flegg, R. H. (1995) *Proteins: Struct., Funct., Genet. 22*, 141−153.
9. Lax, I., Johnson, A., Howk, R., Sap, J., Bellot, F., Winkler, M., Ullrich, A., Vennstrom, B., Schlessinger, J., and Givol, D. (1988) *Mol. Cell. Biol. 8*, 1970−1978.
10. Garrett, T. P. J., McKern, N. M., Lou, M., Frenkel, M. J., Bentley, J. D., Lovrecz, G. O., Elleman, T. C., Cosgrove, L. J., and Ward, C. W. (1998) *Nature 394*, 395−399.
11. Humphrey, P. A., Gangarosa, L. M., Wong, A. J., Archer, G. E., Lund-Johansen, M., Bjerkvig, R., Laerum, O. D., Friedman, H. S., and Bigner, D. D. (1991) *Biochem. Biophys. Res. Commun. 178*, 1413−1420.
12. Kohda, D., Odaka, M., Lax, I., Kawasaki, H., Suzuki, K., Ullrich, A., Schlessinger, J., and Inagaki, F. (1993) *J. Biol. Chem. 268*, 1976−1981.
13. Ullrich, A., Coussens, L., Hayflick, J. S., Dull, T. J., Gray, A., Tam, A. W., Lee, J., Yarden, Y., Libermann, T. A., Schlessinger, J., Downard, J., Mayes, E. L. V., Whittle, N., Waterfield, M. D., and Seeburg, P. H. (1984) *Nature 309*, 418−425.
14. Avivi, A., Lax, I., Ullrich, A., Schlessinger, J., Givol, D., and Morse, B. (1991) *Oncogene 6*, 673−676.
15. Groenen, L. C., Nice, E. C., and Burgess, A. W. (1994) *Growth Factors 11*, 235−257.
16. Kramer, R. H., Lenferink, A. E. G., van Bueren-Koornneef, L., van der Meer, A., van de Poll M. L. M., and van Zoelen, E. J. J. (1994) *J. Biol. Chem. 269*, 8707−8711.
17. van de Poll, M. L. M., Lenferink, A. E. G., van Vugt, M. J. H., Jacobs, J., Janssen, J., Joldersma, M., and van Zoelen, E. J. J. (1995) *J. Biol. Chem. 270*, 22337−22343.
18. Lax, I., Bellot, F., Howk, R., Ullrich, A., Givol, D., and Schlessinger, J. (1989) *EMBO J. 8*, 421−427.
19. Hurwitz, D. R., Emanuel, S. L., Nathan, M. H., Sarver, N., Ullrich, A., Felder, S., Lax, I., and Schlessinger, J. (1991) *J. Biol. Chem. 266*, 22035−22043.
20. Zhou, M., Felder, S., Rubinstein, M., Hurwitz, D. R., Ullrich, A., Lax, I., and Schlessinger, J. (1993) *Biochemistry 32*, 8193−8198.
21. Nice, E. C., Smyth, F., Domagala, T., Fabri, L., Catimel, B., and Burgess, A. W. (1996) *Sci. Tools 1*, 3−5.
22. Domagala, T., Konstantopoulos, N., Smyth, F., Jorissen, R. N., Fabri, L., Geleick, D., Lax, I., Schlessinger, J., Sawyer, W., Howlett, G. J., Burgess, A. W., and Nice, E. C. (2000) *Growth Factors 18*, 11−29.
23. Jorissen, R. N., Epa, V. C., Treutlein, H. R., Garrett, T. P. J., Ward, C. W., and Burgess, A. W. (2000) *Protein Sci. 9*, 310−324.
24. Summerfield, A. E., Hudnall, A. K., Lukas, T. J., Guyer, C. A., and Staros, J. V. (1996) *J. Biol. Chem. 271*, 19656−19659.
25. Wu, D. G., Wang, L. H., Sato, G. H., West, K. A., Harris, W. R., Crabb, J. W., and Sato, J. D. (1989) *J. Biol. Chem. 264*, 17469−17475.
26. Bebbington, C. R., and Hentschel, C. C. G. (1987) in *DNA Cloning* (Glover, D., Ed.) Vol. III, pp 163−188, IRL Press, Oxford, U.K.
27. McKern, N. M., Lou, M., Frenkel, M. J., Verkuylen, A., Bentley, J. D., Lovrecz, G. O., Ivancic, N., Elleman, T. C., Garrett, T. P. J., Cosgrove L., and Ward, C. W. (1997) *Protein Sci. 6*, 2663−2666.
28. Norrander, J., Kempe, T., and Messing, J. (1983) *Gene 26*, 101−106.
29. Carter, P. (1987) *Methods Enzymol. 154*, 382−403.
30. Sanger, F., Nicklen, S., and Coulson, A. R. (1977) *Proc. Natl. Acad. Sci. U.S.A. 74*, 5463−5467.

31. Harlow, E., and Lane, D. (1988) *Antibodies: a Laboratory Manual*, pp 139−243, Cold Spring Harbor Laboratory Publications, Cold Spring Harbor, NY.
32. Gill, G. N., Kawamoto, T., Cochet, C., Le, A., Sato, J. D., Masui, H., McLeod, C., and Mendelsohn, J. (1984) *J. Biol. Chem. 259*, 7755−7760.
33. Stanley, P. (1989) *Mol. Cell. Biol. 9*, 377−383.
34. Nice, E., Lackmann, M., Smyth, F., Fabri, L., Burgess, A. W. (1994) *J. Chromatogr. A660*, 169−185.
35. Catimel, B., Domagala, T., Nerrie, M., Weinstock, J., White, S., Abud, H., Heath, J., and Nice, E. (1999) *Protein Pept. Lett. 6*, 319−340.
36. Catimel, B., Nerrie, M., Lee, F. T., Scott, A. M., Ritter, G., Welt, S., Old, L. J., Burgess, A. W., and Nice, E. C. (1997) *J. Chromatogr. 776*, 15−30.
37. Morton, T. A., and Myszka, D. G. (1998) *Methods Enzymol. 295*, 268−294.
38. Hammacher, A., Simpson, R. J., and Nice, E. C. (1996) *J. Biol. Chem. 271*, 5464−5473.
39. Minton, A. P. (1994) in *Modern Analytical Ultracentrifugation: Acquisition and Interpretation of Data for Biological and Synhtetic Polymer Systems* (Schuster, T. M., and Laue, T. M., Eds.) p 81, Birkhauser, Boston, MA.
40. Bishayee, S. (2000) *Biochem. Pharmacol. 60*, 1217−1223.
41. De Crescenzo, G., Grothe, S., Lortie, R., Debanne, M. T., and O'Connor-McCourt, M. (2000) *Biochemistry 39*, 9466−9476.
42. Nice, E. C., and Catimel, B. (1999) *BioEssays 21*, 339−352.
43. Mendelsohn, J. (1989) in *Cancer Cells* (Furth, M., and Greaves, M., Eds.) pp 395−462, Cold Spring Harbor Laboratory Press, Cold Spring Harbor, NY.
44. Grimaux, M., Laine-Bidron, C., and Magdelenat, H. (1989) *Tumor Biol. 10*, 215−224.
45. Brown, P. M., Debanne, M. T., Grothe, S., Bergsma, D., Caron, M., Kay, C., and O'Connor-McCourt, M. D. (1994) *Eur. J. Biochem. 225*, 223−233.
46. Greenfield, C., Hiles, I., Waterfield, M. D., Federwisch, M., Wollmer, A., Blundell, T. L., and McDonald, N. (1989) *EMBO J. 8*, 4115−4123.
47. Lax, I., Mitra, A. K., Ravera, C., Hurwitz, D. R., Rubenstein, M., Ullrich, A., Stroud, R. M., and Schlessinger, J. (1991) *J. Biol. Chem. 266*, 13828−13833.
48. Lemmon, M. A., Bu, Z. M., Ladbury, J. E., Zhou, M., Pinchasi, D., Lax, I., Engelman, D. M., and Schlessinger, J. (1997) *EMBO J. 16*, 281−294.
49. Odaka, M., Kohda, D., Lax, I., Schlessinger, J., and Inagaki, F. (1997) *J. Biochem. 122*, 116−121.
50. Tanner, K. G., and Kyte, J. (1999) *J. Biol. Chem. 274*, 35985−35990.
51. Saxon, M. L., and Lee, D. C. (1999) *J. Biol. Chem. 274*, 28356−28362.
52. Tzahar, E., Pinkas-Kramarski, R., Moyer, J. D., Klapper, L. N., Alroy, I., Levkowitz, G., Shelly, M., Henis, S., Eisenstein, M., Ratzkin, B. J., Sela, M., Andrews, G. C., and Yarden, Y. (1997) *EMBO J. 16*, 4938−4950.
53. Baselga, J., Pfister, D., Cooper, M. R., Cohen, R., Burtness, B., Bos, M., D'Andrea, G., Seidman, A., Norton, L., Gunnett, K., Falcey, J., Anderson, V., Waksal, H., and Mendelsohn, J. (2000) *J. Clin. Oncol. 18*, 904−914.

BI010037B